Ultrafast formation of ANFs with kinetic advantage and new insight in mechanism

Lianqing Huang[a], Meiyun Zhang [a, *], Jingyi Nie[a, *], Bin Yang [a, *], Jiaojun Tan[a], Shunxi Song[a]

a College of Bioresources Chemical and Materials Engineering, Shaanxi Province Key Laboratory of Papermaking Technology and Specialty Paper, National Demonstration Center for Experimental Light Chemistry Engineering Education, Key Laboratory of Paper-Based Functional Materials of China National Light Industry, Shaanxi University of Science & Technology, Xi·an 710021, China

* Corresponding author.

E-mail addresses: niejingyi@sust.edu.cn (J. Nie), mymyzhang@sust.edu.cn (M. Zhang).

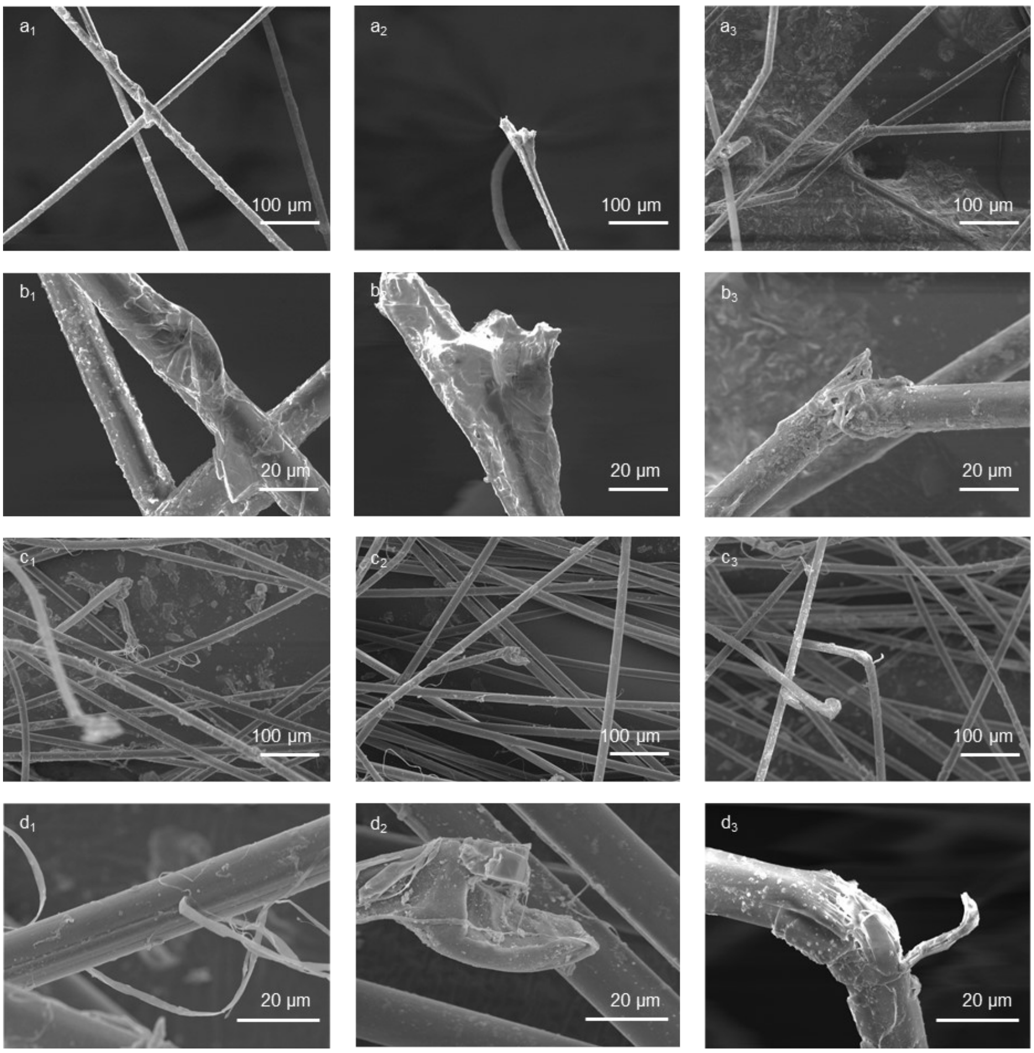

Figure S1. Microstructure of fiber pretreated by alkali solution. (a) Unwashed fibers and (c) washed fibers which were pretreated with alkaline solution. (b) and (d) were zoom images, respectively.

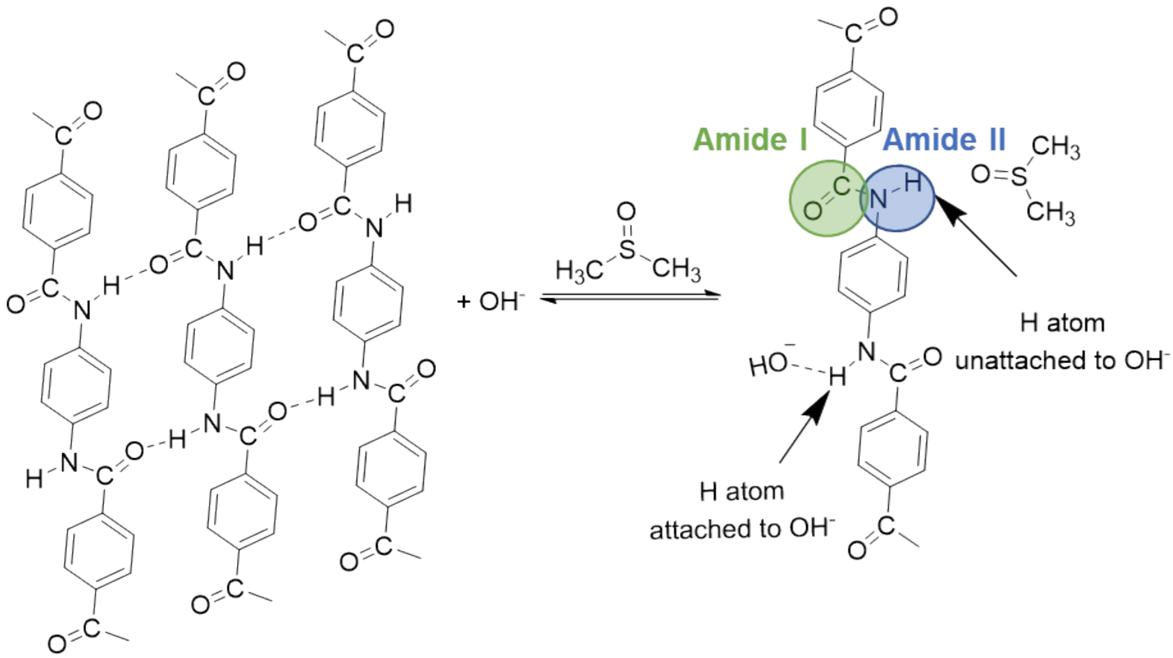

Figure S2. Hypothesis of the formation of ANFs.

Table S1. Different mass ratios of KOH to aramid fibers

Volume of H_2O (ml)	Mass of KOH (g)	KOH: Aramid fibers (g:g)	Concentration of KOH in H_2O ($g \cdot ml^{-1}$)	Volume of DMSO (ml)	Concentration of ANFs (*wt* %)
2	0.05	1:2	0.025	50	0.2
2	0.1	2:2	0.05	50	0.2
2	0.15	3:2	0.075	50	0.2
2	0.2	4:2	0.1	50	0.2
2	0.25	5:2	0.125	50	0.2

Table S2. Different volume ratios of H_2O to DMSO

Volume of H_2O (ml)	Volume percentage	Mass of KOH (g)	Concentration of KOH in H_2O ($g\ ml^{-1}$)	Volume of DMSO (ml)	Concentration of ANFs (*wt* %)
0.5	1%	0.15	0.3	50	0.2
1	2%	0.15	0.15	50	0.2
1.5	3%	0.15	0.1	50	0.2
2	4%	0.15	0.075	50	0.2
2.5	5%	0.15	0.06	50	0.2

Table S3. Summary of ANFs preparation methods

Preparation Method	Concentration	Diameter of ANFs	Energy Consumption	Operability	Preparation time	Ref.
Polymerization induced self-assembly	3 *wt*%	20-50 nm	Low	Low		[1]
Electrospinning	-	275 nm-15 μm	High	Low	-	[2]
Immersion Rotary Jet-Spinning	-	500-1000 nm	Medium	Low	-	[3]
Mechanical Disintegration	1 *wt*%	10-200 nm	High	Low	-	[4]
Deprotonation	0.2 *wt*%	3-30 nm	Low	High	7 days	[5]
Proton donor-assisted	0.2 *wt*%	10-12 nm	Low	High	4 h	[6]
monomer-to-ANFs synthesis	0.2 *wt*%	122 nm (DLS-determined size)	Low	High	15 h	[7]
Sol-Group	0.2 *wt*%	10-20 nm	Low	High	20 min	This work
Pre-Group	0.2 *wt*%	10-20 nm	Low	High	10 min	This work

Table S4. Wavenumbers and vibration types of aramid fibers and ANFs in Raman scattering.

Aramid fiber	ANFs/DMSO	Assignment/%	Shift
	950, 1047, 1423	DMSO	Appear
1183	1159	Ring C-H in-plane bending	shift
1276	1263	N-H in-plane bending, ring C-H stretching	shift
1324	1356	Ring C-H in-plane bending, N-H in-plane bending	shift
1400	1431	Ring C-H in-plane bending, ring C-C stretching	shift
1509	1535	ring C-H in-plane bending, ring C-C stretching	shift
1611	1606	ring C-C stretching, C=O stretching	shift
1650		C=O stretching B, N-C stretching	Disappear

Table S5. Wavenumbers and vibration types of aramid fibers and ANFs in FT-IR scattering.

Aramid fiber	ANFs/DMSO	Assignment	Shift
	1020	DMSO	Appear
	1423	DMSO	Appear
819	831	C-H aromatic ring	Shift
864	900	Ring C-H out-of-plane bending	Shift
964	950	Ring C-H and N-H in-plane bending	Shift
1103	1065	Ring C-H and N-H in-plane bending	Shift
1299	1309	Ring C-C, C-N and N-H vibration	Shift
1395	1413	Ring C-H, N-H and C-H in-plane bending, ring vibration	Shift
1608	1653	C-C, N-C and C-H in-plane bending	Shift
1670	1653	Amide I	Shift
1538		Amide II	Disappear

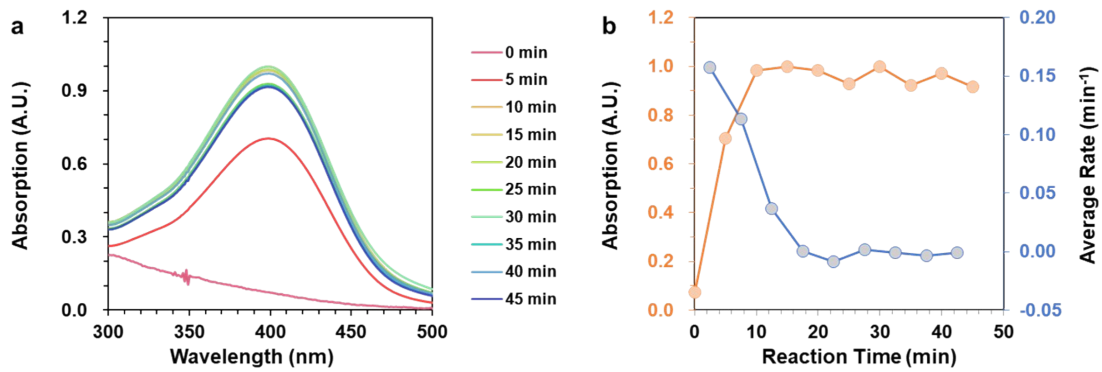

Figure S3. UV-Vis absorption and reaction rate of ANFs with different time when mass radios of KOH to aramid fibers was 1:2.

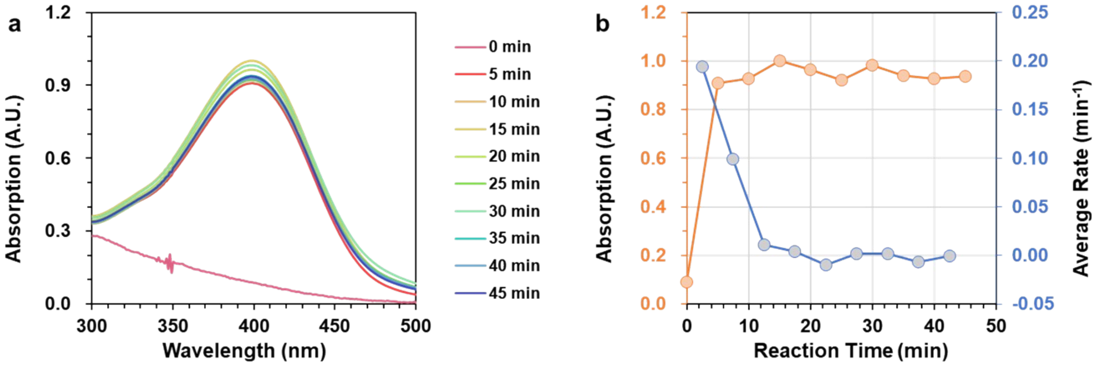

Figure S4. UV-Vis absorption and reaction rate of ANFs with different time when mass radios of KOH to aramid fibers was 2:2.

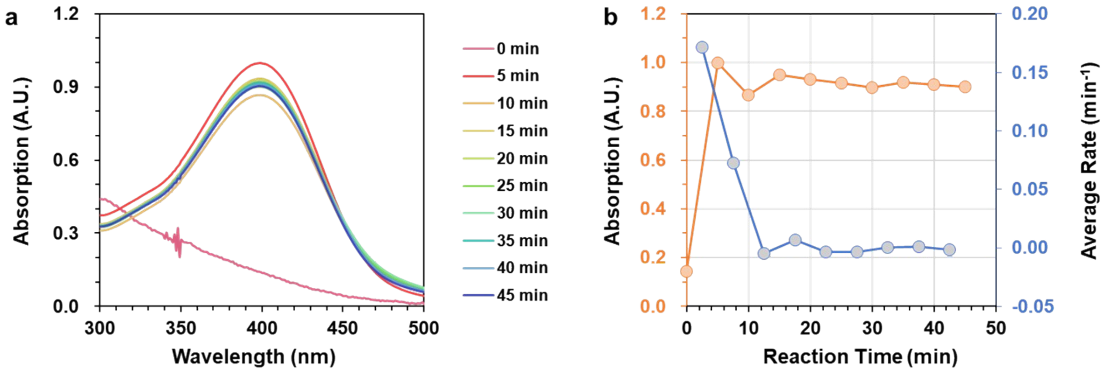

Figure S5. UV-Vis absorption and reaction rate of ANFs with different time when mass radios of KOH to aramid fibers was 3:2.

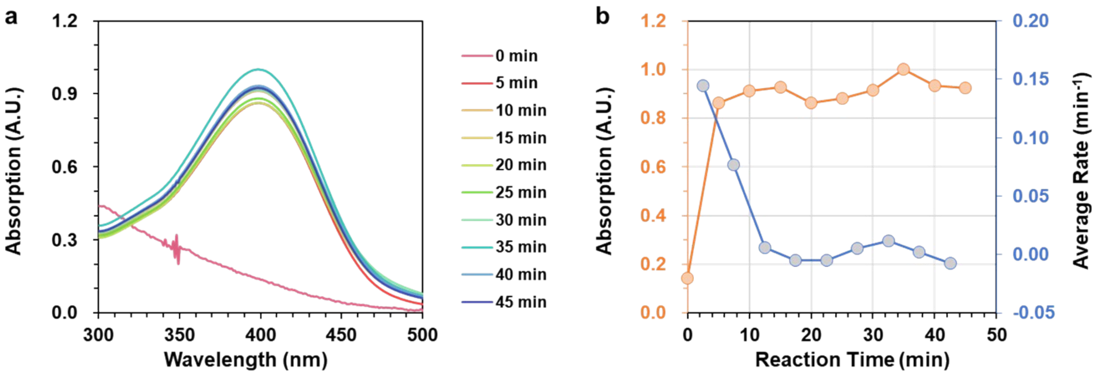

Figure S6. UV-Vis absorption and reaction rate of ANFs with different time when mass radios of KOH to aramid fibers was 4:2.

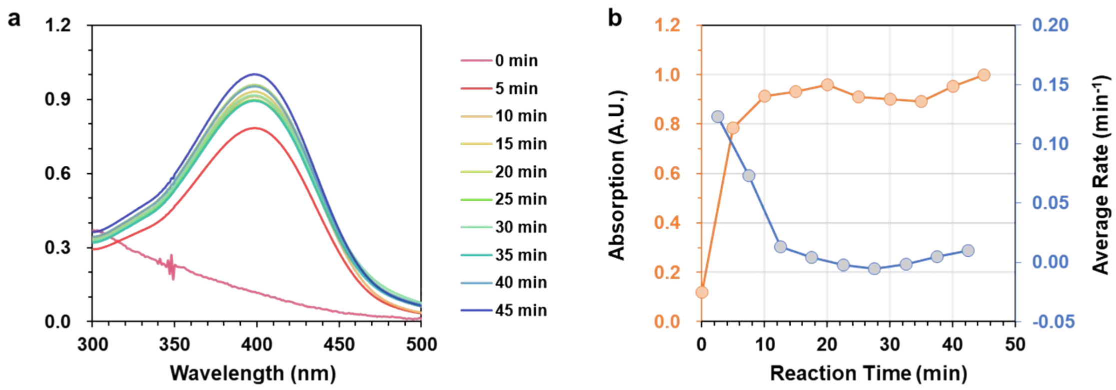

Figure S7. UV-Vis absorption and reaction rate of ANFs with different time when mass radios of KOH to aramid fibers was 5:2.

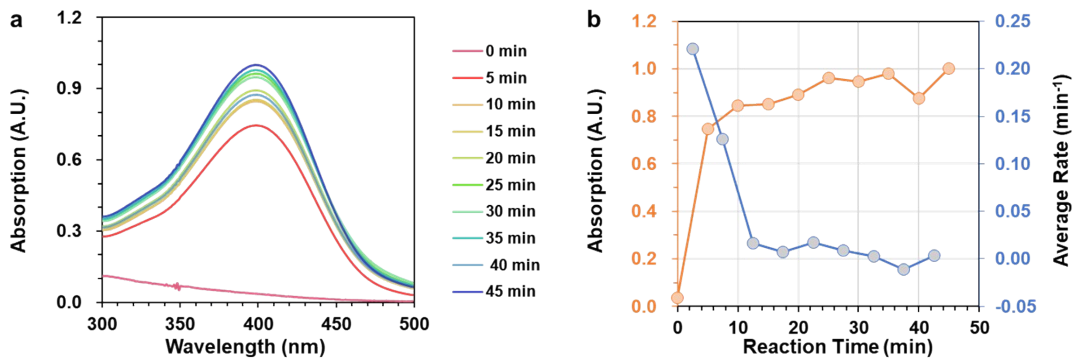

Figure S8. UV-Vis absorption and reaction rate of ANFs with different time when volume radios of H_2O to DMSO was 1%.

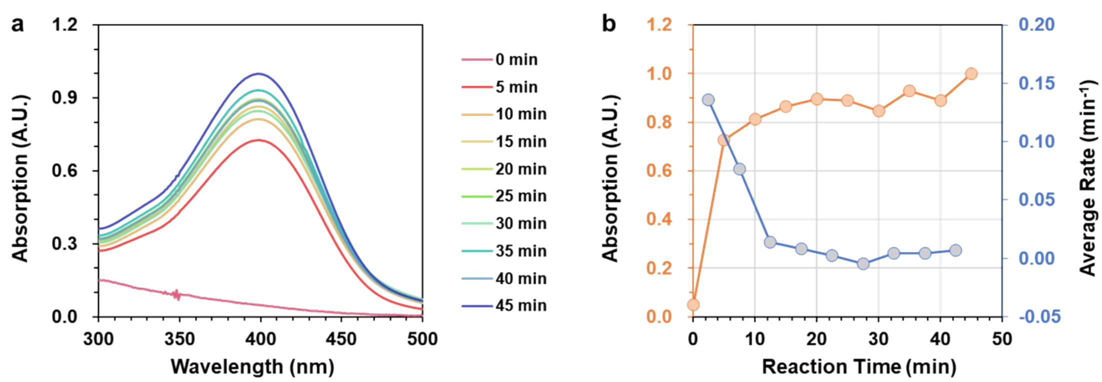

Figure S9. UV-Vis absorption and reaction rate of ANFs with different time when volume radios of H_2O to DMSO was 2%.

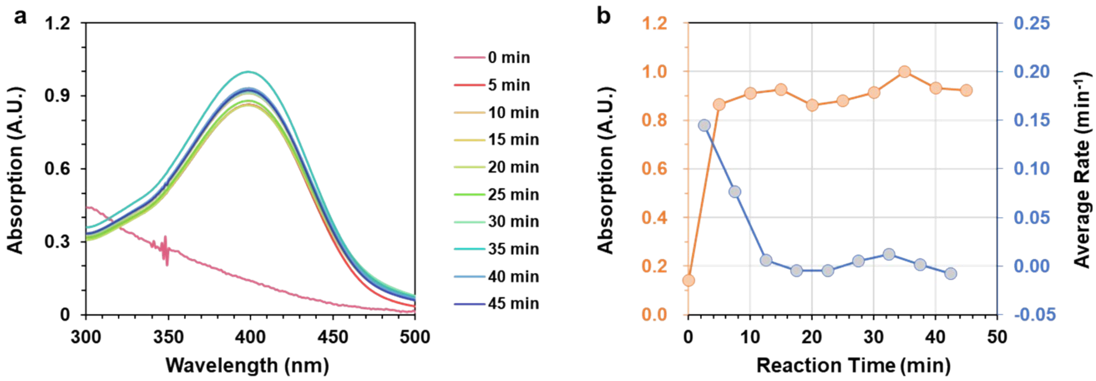

Figure S10. UV-Vis absorption and reaction rate of ANFs with different time when volume radios of H_2O to DMSO was 3%.

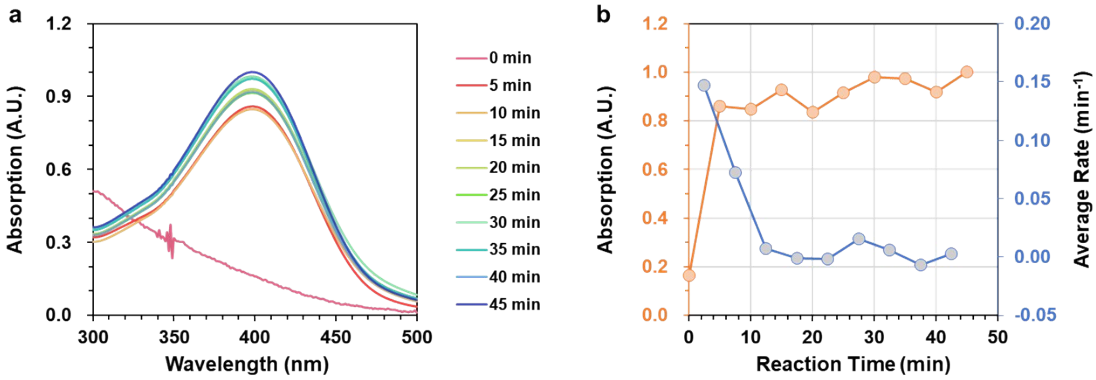

Figure S11. UV-Vis absorption and reaction rate of ANFs with different time when volume radios of H_2O to DMSO was 4%.

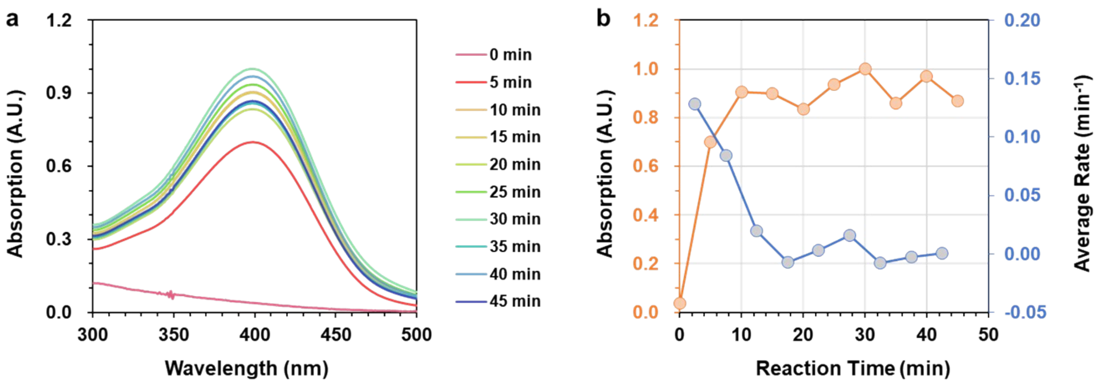

Figure S12. UV-Vis absorption and reaction rate of ANFs with different time when volume radios of H_2O to DMSO was 5%

$$\delta_{mix} = \varphi_1 \cdot \delta_1 + \varphi_2 \cdot \delta_2 \quad \text{(Equ 1)}$$

$$|\delta_{mix} - \delta_{ANFs}| \to 0 \quad \text{(Equ 2)}$$

δ_{mix} represents the solubility coefficient of the mixing system, δ_1 and δ_2 respectively represent the solubility coefficient of the two components in the mixing system, φ_1 and φ_2 respectively represent the mole fraction of the two components in the mixing system. If δ_{Mix} is close to δ_{ANFs}, the compatibility between the two components is better and the system is more stable。

Reference

1. H. C. Yan, J. L. Li, W. T. Tian, L. Y. He, X. L. Tuo and T. Qiu, *RSC Adv.*, 2016, **6**, 26599-26605.
2. J. Yao, J. Jin, E. Lepore, N. M. Pugno, C. W. M. Bastiaansen and T. Peijs, *Macromol. Mater. Eng.*, 2015, **300**, 1238-1245.
3. G. M. Gonzalez, L. A. MacQueen, J. U. Lind, S. A. Fitzgibbons, C. O. Chantre, I. Huggler, H. M. Golecki, J. A. Goss and K. K. Parker, *Macromol. Mater. Eng.*, 2017, **302**.
4. S. Ifuku, H. Maeta, H. Izawa, M. Morimoto and H. Saimoto, *RSC Adv.*, 2014, **4**, 40377-40380.
5. M. Yang, K. Cao, L. Sui, Y. Qi, J. Zhu, A. Waas, E. M. Arruda, J. Kieffer, M. D. Thouless and N. A. Kotov, *ACS Nano*, 2011, **5**, 6945-6954.
6. B. Yang, L. Wang, M. Zhang, J. Luo and X. Ding, *ACS Nano*, 2019, **13**, 7886-7897.
7. J. M. Koo, H. Kim, M. Lee, S. A. Park, H. Jeon, S. H. Shin, S. M. Kim, H. G. Cha, J. Jegal, B. S. Kim, B. G. Choi, S. Y. Hwang, D. X. Oh and J. Park, *Macromolecules*, 2019, **52**, 923-934.